ELSEVIER

Earth and Planetary Science Letters 184 (2001) 623–633

EPSL

www.elsevier.com/locate/epsl

Effect of isostatic rebound on modelled ice volume variations during the last 200 kyr

Michel Crucifix [a,*], Marie-France Loutre [a], Kurt Lambeck [b], André Berger [a]

[a] *Institut d'Astronomie et de Géophysique G. Lemaître, Université catholique de Louvain, 2 Chemin du Cyclotron, B-1348 Louvain-la-Neuve, Belgium*

[b] *Research School of Earth Sciences, Institute of Advanced Studies, The Australian National University, Mills Road, Canberra, A.C.T. 0200, Australia*

Received 11 July 2000; accepted 23 November 2000

Abstract

Deformation of the lithosphere under an ice load can be approximated using the hypothesis of local damped isostasy. This simple formulation has been systematically compared with a three-dimensional model of the crust–mantle system for simple ice-load scenarios with a period in the range 20–100 kyr. The comparison enables us to introduce the concepts of effective upper mantle density and effective relaxation time into the isostatic model for the response of the Earth to the ice sheets. These parameters depend on the Earth model considered, ice sheet size and the period of the load cycle. The local damped isostasy model has been implemented in the Louvain-la-Neuve climate model to assess the impact of isostasy on continental ice volume variations for the last 200 kyr. Results suggest that isostasy acts as a negative feedback for ice volume during the glaciation process and acts as a positive feedback during the deglaciation. Moreover, taking isostasy into account is necessary to simulate variations in Northern Hemisphere ice volume during isotopic stage 3. Lastly, the use of effective mantle density and effective relaxation time improves the model performance regarding SPECMAP reconstructions.

Keywords: glacial rebound; cycles; climate; models

1. Introduction

Previous model studies suggest that the viscoelastic response of bedrock to the ice load is an important process to explain the long term variability of climate, and in particular the 100 kyr cycle that characterized the last half of the Pleistocene climate. For example, Oerlemans [1] studied the effect of isostasy on climate with a vertically integrated ice sheet model and local damped isostasy in which net accumulation rate is calculated following the equilibrium line concept. In this model, a relaxation time of 10 kyr for bedrock response produces a 100 kyr glacial cycle with a sawtooth shape in response to astronomical forcing. Oerlemans suggested that this 100 kyr cycle is internally generated. Hence, the orbital forcing should be considered as a stimulat-

* Corresponding author. Tel.: +32-10-473365; Fax: +32-10-474722; E-mail: crucifix@astr.ucl.ac.be

0012-821X/01/$ – see front matter
PII: S0012-821X(00)00361-7

ing agent for free oscillations of the system. Moreover, by using an isostatic adjustment time scale of 3 kyr so that the isostatic balance is quickly restored, large ice sheets cannot grow. This hypothesis that lithosphere dynamics can induce 100 kyr internal variability was also addressed by Ghil and Le Treut [2,3] with a zero-dimensional model of the climate represented by a system of three equations, including bedrock deflection under ice load. In contrast to Oerlemans, their results suggest that the bedrock does not affect fundamentally the internal variability of the climate system but when orbital forcing is applied, the crustal deformation enhances the response of the system at 1/19 kyr^{-1}−1/23 kyr^{-1} = 1/109 kyr^{-1}. Hence, the bedrock deflection should be considered as an important element for the non-linear resonance of the system to precessional frequencies rather than as a source of internal variability. This aspect was further investigated with a one-dimensional ice sheet–bedrock model by Birchfield and Ghil [4]. In this model, the net accumulation is a linear function of surface temperature that depends on altitude and latitude. They confirmed that isostatic rebound enhances the suborbital response and its variations during the Pleistocene but that it is not an important source of internal variability in climate.

The most detailed assessment of isostasy impact on the 100 kyr cycle using a coupled model of the atmosphere–cryosphere system was published by Tarasov and Peltier [5]. In that study, a one-level non-linear spectral energy balance model of the atmosphere was coupled to an ice sheet model based on the shallow-ice approximation. The authors demonstrated that ice volume change during the deglaciation is strongly dependent on isostasy. In particular, when eliminating bedrock response entirely, more than 65% of the Last Glacial Maximum (LGM) continental ice volume remains during the Holocene. Similarly, a too short relaxation time (1 kyr) leads to overestimation of ice volume during the Holocene.

The purpose of this article is to examine in detail the effect of the climate–lithosphere interaction on the ice volume variations over the last 200 kyr. This work had therefore to be performed with a model including the atmosphere, the hydrosphere, the cryosphere and the lithosphere. Being given the limits of present-day general circulation models, the model used here is consequently a model of intermediate complexity, allowing fast computing to perform several sensitivity experiments. The sectorial climate–ice sheet model of Louvain-la-Neuve (LLN 2D NH model [6,7], a brief description of which is given in Appendix A) appears to be a suitable tool. Its computing cost is quite low (about 300 kyr per CPU day) and it has been shown to reproduce with reasonable accuracy the ice sheet volume variations throughout the last four glacial–interglacial cycles [8,9] in response to astronomical forcing and CO_2 variations.

The climate–lithosphere interaction in the LLN model assumes the hypothesis of local damped isostasy over a hydrostatic asthenosphere which is based on the following equation: let ρ_i and ρ_a be the densities of ice and of the asthenosphere, respectively, τ the relaxation time and b_0 the unperturbed bedrock altitude. The bedrock altitude b under an ice column of local thickness H is governed by the following differential equation:

$$\frac{\partial b}{\partial t} = -\frac{1}{\tau}\left[(b-b_0) + \frac{\rho_i}{\rho_a}H\right] \quad (1)$$

This equation is solved explicitly with a time step of 1 kyr. The variables b, b_0 and H are latitude dependent, the meridional resolution being 0.5°.

Tarasov and Peltier [5,10] have already compared this simple isostasy model with an explicit two-dimensional (2-D) viscoelastic formulation of the lithosphere–mantle system. They showed that local isostasy is a valid approach for representing lithosphere–climate interactions in the context of 100 kyr cycle climate models. The main limitation of its local character is that it can induce local over- and underestimations of the lithosphere response to ice load when compared with a 2-D viscoelastic model [11].

Parameter values used by different authors are summarized in Table 1. Depending on the author, density varies from 2700 kg/m^3 to 3300 kg/m^3 and the relaxation time varies from 3 kyr to 12 kyr.

Table 1
Values of the density of the asthenosphere (ρ_a) and the relaxation time (τ) used by several authors

Reference	ρ_a (kg/m^3)	τ (kyr)
Oerlemans, 1980 [1]	2700[a]	5–11
Tarasov and Peltier, 1997 [5]	3300	5
LeMeur and Huybrechts, 1996 [11]	3300	3
Peltier and Marshall, 1995 [29]	3300	3
Birchfield and Ghil, 1981 [30]	2800	3
Neeman at al., 1988 [31]	3200	12

[a]Oerlemans indicates an asthenosphere density of three times ice density.

Besides, Birchfield and Ghil [4] used in their ice sheet–bedrock model a perfectly elastic lithosphere over a very deep viscous mantle of density 5500 kg/m^3. However, we argue that nominal values are inappropriate in most cases. Indeed, the model (Eq. 1) assumes a crustal response whose magnitude is determined by the condition of local isostatic equilibrium but which lags behind the variations of the load H. For loads characterized by short periods (i.e. of the order of 20 kyr), or for loads of small size (i.e. characterized by short wavelength), the equilibrium limit is not necessarily achieved at any time so that if a nominal sublithospheric density is used in Eq. 1 the rate of change in the bedrock altitude is likely to be overestimated. Hence some depth-averaged value for the density is required. This value will be a function of both the size of the ice sheet and the period of the cyclic loading. Likewise, because different ice sheet sizes stress the mantle down to different depths, the time constant can also be expected to depend on the ice sheet size and the cycle period, particularly when the mantle viscosity is depth dependent.

Therefore, in this paper we first compare the locally damped isostatic model (Eq. 1) with a more realistic viscoelastic model of the lithosphere–mantle system to estimate effective values for ρ_a and τ that are appropriate for Eq. 1 (Section 2). Secondly, we use these effective parameters in the climate model to explore the dependence of the ice volume estimate during the last 200 kyr on isostatic response of the Earth (Section 3). The discussion of results and conclusions are given in Section 4.

2. Effective parameters for the local damped isostatic equation

The damped isostatic displacement is first compared with the response of the three-dimensional (3-D) viscoelastic model of the crust–mantle system [12] for simple ice-load scenarios. In this geophysical model, the Earth is represented as the superposition of compressible Maxwell body layers of given elasticity and viscosity. The elastic moduli depth profiles are taken from Dziewonski and Anderson [13]. The lithosphere is 65 km thick and is effectively elastic. An upper mantle extends to 650 km depth with an effective viscosity of 4×10^{20} Pa s, and the lower mantle has an effective viscosity of 10^{22} Pa s. This profile has been shown to model adequately the mantle response under ice and water in regions where sea level data are sufficient to constrain model parameters, such as the Australian margin, Fennoscandia, the North Sea and the British Isles [14–16]. In North America, some studies have suggested that the lower mantle viscosity may be less than assumed above (e.g. viscosity profile VM2 in [10]) but other studies, using rotational constraints, gravity as well as sea level data from North America, support the profile used here [17–19].

The following ice-load scenarios have been applied as external forcing to the 3-D geophysical model. An axi-symmetric ice sheet of radius r and double-parabolic height profile grows so that its altitude at summit increases linearly during a time $0.9P$, P being an arbitrary time interval. This altitude then decreases linearly until zero over a time interval $0.1P$. The model predictions for the isostatic displacement of the crust at the center of the ice load are then compared with the approximate formulation (Eq. 1) and the parameters ρ_a and τ are estimated using a chi-square optimization method.

Fig. 1a summarizes the effective mantle density ρ_a for cyclic loads with periods of 20, 40 and 100 kyr and ice sheets of radius ranging from 250 to 2000 km. For a given period of cycling loading, the effective density increases with increasing load radius for $r \gtrsim 500$ km. This tendency reflects (a) the increasing density of the mantle with depth and (b) the fact that the restor-

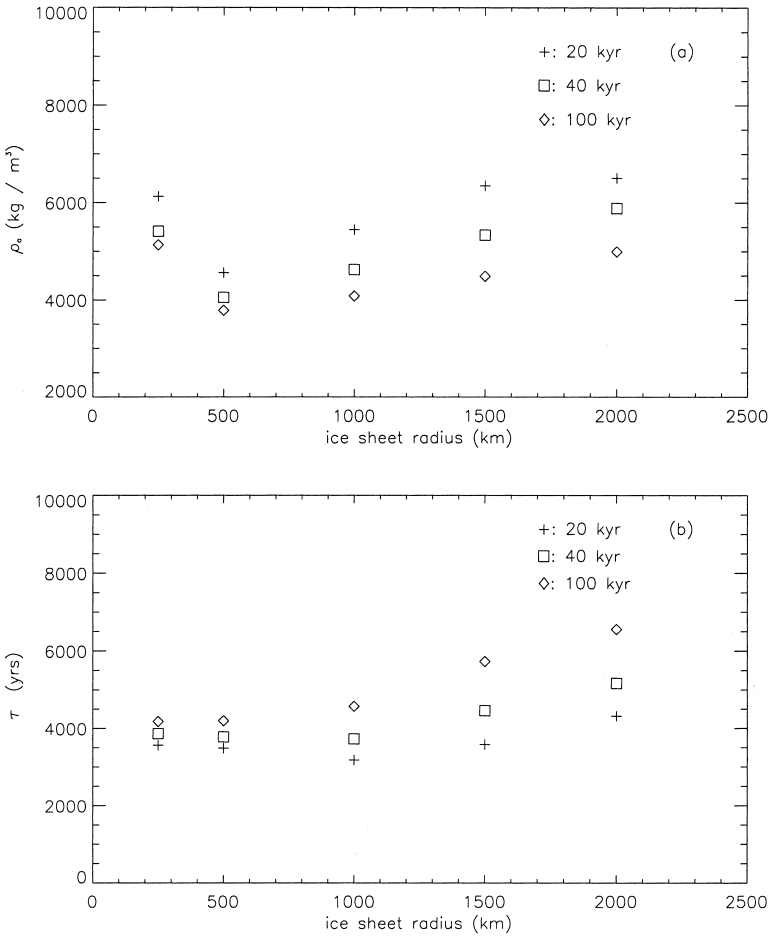

Fig. 1. Effective mantle parameters ρ_a (a) and τ (b) to be applied to the local isostatic formulation to give a best fit to lithospheric displacement simulated with the 3-D viscoelastic Earth model discussed in Section 2 for various loading periods.

ing force induced by the radial displacement of surfaces of equal density in the viscous mantle is proportional to density. For small radius loads, the response is controlled mainly by the flexural strength of the lithosphere and the radial displacement is much less than predicted by the local isostatic assumption (Eq. 1). Hence the effective density in Eq. 1 now increases with decreasing load radius. When the ice sheet radius is fixed, the effective density decreases when the period increases (Fig. 1a). For very long load periods (i.e. ≥ 100 kyr), the effective density approaches its 'actual' value of about 3500 kg/m^3 because time allows the local isostatic condition to be reached.

Fig. 1b illustrates the dependence of the effective time constant τ on load radius and load cycle. In this case τ generally increases with load radius because large ice sheets impact deeper mantle layers which are more viscous. For small load radius and short period, the ice load is supported mainly by the elasticity of the lithosphere. When the load radius increases, the lithosphere plays a decreasing role and this tends to decrease the effective relaxation time. When the load radius increases further, the lower mantle begins to be increasingly stressed and τ now increases with load radius as the viscous lower mantle participates increasingly in the relaxation. For the longest

cycle load period (i.e. 100 kyr), effective relaxation time always increases with increasing load radius because the effect of increasing mantle viscosity with depth dominates that of the lithosphere, even for short load radius.

3. Effect of mantle isostasy on climate

3.1. Experimental setup

The LLN 2D NH ice sheet climate model was used to simulate the time evolution of the three major ice sheets in the Northern Hemisphere (NH), i.e. Greenland, Northern American and Eurasian (British Isles and Fennoscandia) ice sheets. The model is run for the last 200 kyr and is forced by the seasonal cycle of insolation [20] and by CO_2 atmospheric concentration reconstructed from the Vostok ice core [21]. Initial conditions are no pre-existing ice and bedrock altitude corresponding to its unperturbed state. Sensitivity studies with this model showed that initial conditions influence the simulated ice volume for approximately the last 60 kyr [8] so that the prediction for only the last 140 kyr or so should be considered.

Three simulations have been considered. In the first experiment (NoI), no isostatic rebound is included. In this case the bedrock altitude keeps its initial value during the entire experiment, whatever the simulated ice volume. In the second experiment (NOM), the local damped formulation (Eq. 1) is implemented with nominal values, i.e. an asthenosphere density of $\rho_a = 3000$ kg/m^3 and a relaxation time of $\tau = 4000$ yr (cf. [10]). The third experiment (EFF) uses the local damped isostasy formulation with effective parameters computed in Section 2 applied independently for each ice sheet, depending on their mean size. The adopted values are summarized in Table 2.

Table 2
Effective upper mantle density (ρ_a) and relaxation time (τ) applied independently to each ice sheet in experiment EFF

Ice sheet	Radius (km)	ρ_a (kg/m^3)	τ (yr)
Greenland	1000	5000	3750
N. America	1500	5500	4500
Eurasia	1500	5500	4500
Nominal	–	3000	4000

Effective parameters depend on the mean radius of the ice sheet and on the viscosity depth profile. The assumed load–unload cycle is 40 kyr. Nominal parameters are displayed for comparison.

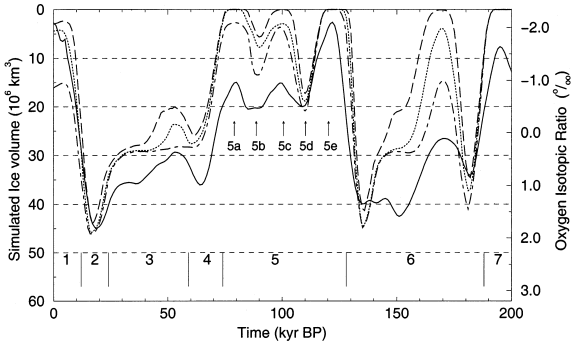

Fig. 2. Ice volume simulated by the LLN model over the last 200 kyr for different sets of parameters in the local damped isostasy formulation: no isostasy (dot-dashed line), nominal isostasy (dashed line) and effective isostasy (dotted line). Ice volume is compared with oxygen isotopic ratio (full line, RHS scale) from SPECMAP. The scales were adjusted such that LGM and present oxygen isotopic ratios correspond to ice volumes of 45×10^6 km^3 at the LGM and to 3×10^6 km^3 at the present-day. The ages of isotopic stage transitions are indicated [32].

3.2. Results

Fig. 2 displays the time evolution of total continental ice volume in the NH simulated during the last 200 kyr for the three experiments. Simulated ice volumes are compared with global δ^{18}O reconstruction from SPECMAP [22]. Although these global δ^{18}O proxy data should not be considered as an absolute indicator of continental ice volume, they provide a useful guideline for assessing the quality of the simulations.

3.2.1. No isostasy experiment (NoI)

The model is able to simulate two distinct glacial–interglacial cycles over the last 200 kyr when no isostasy is introduced. However, major discrepancies with the SPECMAP reconstruction occur. The main problem is the incomplete melting of the Northern American and Eurasian ice sheets between the LGM (isotopic stage 2) and the Holocene. Namely, there is 16×10^6 km^3 of ice left in

Table 3
Continental ice volume in the NH, expressed in 10^6 km^3, at the end of the 200 kyr experiments (this corresponds to the present-day)

Ice sheet	NoI	NOM	EFF
Greenland	6.1	3.0	3.9
N. America	7.2	0.0	0.2
Eurasia	2.6	0.0	0.2
Total	16.0	3.0	4.3

Results are given for experiments NoI (no isostasy), NOM (isostasy with nominal parameters) and EFF (isostasy with effective parameters).

the NH at the present-day, which is distributed as follows (see also Table 3): 6.1×10^6 km^3 over Greenland, 7.2×10^6 km^3 over Northern America and 2.6×10^6 km^3 over Eurasia. This behavior is consistent with the results from Tarasov and Peltier [5] which also show only a partial melting of the continental ice at the Holocene when no bedrock response is introduced. There are also other substantial discrepancies between the NoI experiment and the SPECMAP reconstruction. First, NoI is unable to reproduce sufficient continental ice volume variations to characterize isotopic stage 3 (OIS 3), i.e. a decrease after OIS 4 (64 kyr BP) and an increase between 55 kyr BP and 45 kyr BP. Second, ice volume is underestimated between 100 kyr BP and 70 kyr BP (OIS 5d to 5b). This feature is a known weakness of the LLN model related to the complete melting of Greenland spuriously simulated during the last interglacial (OIS 5e) [8]. But when no isostatic rebound is included, the model simulates variations in ice volume of the order of 10×10^6 km^3 between 100 kyr BP and 70 kyr BP and the amplitudes of these variations are clearly overestimated.

3.2.2. *Damped isostasy with nominal parameters (NOM)*

Experiment NOM, corresponding to a local damped isostatic formulation with nominal parameters, also shows clearly two glacial–interglacial cycles. The timing of ice volume variations is roughly the same as in NoI but the amplitude of the variations differs. During periods characterized by a decrease in ice volume, ice volume decreases more rapidly in NOM than in NoI. Besides, during periods characterized by an increase in ice volume, ice volume increases less in NOM than in NoI. Both features have generally favorable consequences on the simulated ice volume. First, NOM is able to represent the present-day interglacial, the Northern American and the Eurasian ice sheets having completely disappeared at the present-day and 3.0×10^6 km^3 of ice remaining over Greenland, consistent with present-day estimates. However, the simulated melting rate between the LGM and the Holocene is likely to be overestimated. Besides, the model is able to predict rates of change in ice volume during OIS 3 and OIS 5b to 5d that are more consistent with SPECMAP than NoI.

3.2.3. *Damped isostasy with effective parameters (EFF)*

The ice volume simulated with effective parameters computed in Section 2 lies between the ice volumes simulated with no isostasy (NoI) and with isostasy using nominal parameters (NOM). With respect to NOM, the ice volume increases slightly more rapidly during periods when ice volume increases (e.g. before 110 kyr BP), but it decreases less after 110 kyr BP. Consequently there is always more ice in experiment EFF than in NOM. When compared to the other experiments, the amplitude of ice volume variations simulated in EFF shows generally the best agreement with SPECMAP. Indeed, by contrast to NoI, a clear transition is simulated between the LGM and the Holocene period, with only an amount of 4.75×10^3 km^3 of ice remaining at the present-day. However, this deglaciation is less abrupt than in NOM. On the other hand, the model with effective parameters does reproduce rates of change of ice volume during OIS 3 and OIS 5 that are certainly better than in the no isostasy case. Furthermore, EFF avoids the complete ice melting simulated in NOM at 100 kyr BP, but the decrease in ice volume associated with the transition between OIS 5d and OIS 5c remains overestimated.

In order to determine the respective impacts of effective density and relaxation time on this improvement with respect to the NOM experiment,

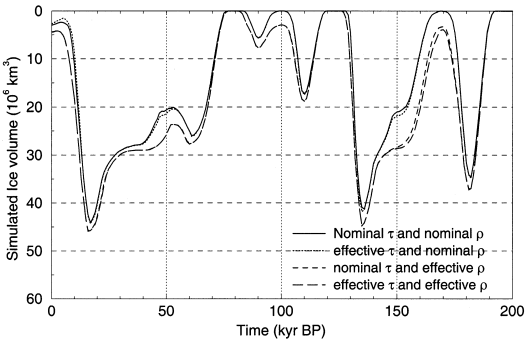

Fig. 3. Ice volume simulated by the LLN model over the last 200 kyr with (a) nominal relaxation time and density, (b) effective relaxation time and nominal density, (c) nominal relaxation time and effective density, and (d) effective relaxation time and effective density.

two additional experiments were performed. The first one uses effective density, fixed as in EFF, and a relaxation time of 4000 yr. The second experiment uses nominal density and effective relaxation time (Fig. 3). From these experiments, it readily appears that density is the key parameter and relaxation time has generally minor influence. A careful analysis reveals that using effective relaxation time has, however, a non-negligible impact on the last deglaciation. Indeed, Eurasian and North American ice sheets melt slightly more rapidly with effective relaxation times than with nominal values. The difference between the simulated ice volumes of both ice sheets between the two experiments amounts to 2.3×10^6 km^3 at 11 kyr BP. As will be discussed in Section 4, this is a direct consequence of the fact that the bedrock takes more time to recover its equilibrium altitude in the effective parameter case. Although Greenland's effective relaxation time is slightly shorter than the nominal one, it melts more rapidly as well because it simply follows the global warming trend induced by the biggest ice sheets.

3.2.4. *Spectral analysis*

The Multi-Taper-Method (MTM, [23]) has been used to calculate the spectrum and *F*-test values of the NoI, NOM and EFF ice volumes (Fig. 4). This MTM analysis provides complementary information concerning the effect of isostasy on the climate response to insolation and CO_2 forcings. In particular, it appears that isostatic rebound does not significantly modify the amplitude of ice variations at frequencies of 41 kyr^{-1} and 23 kyr^{-1}. Although some modification in amplitude occurs at longer periods, this is not significant at the 95% probability level because of the limited time span of our integration. Thus it is not possible to confirm here that bedrock isostasy enhances the suborbital response (e.g. periods of 55.2 and 94.7 kyr) of ice volume as earlier suggested [4]. This specific question should be addressed in the context of 400 kyr simulations, now made possible as a reconstruction of atmospheric CO_2 over that period is now available [24].

4. Discussion

The sensitivity experiments carried out here confirm the importance of introducing isostasy

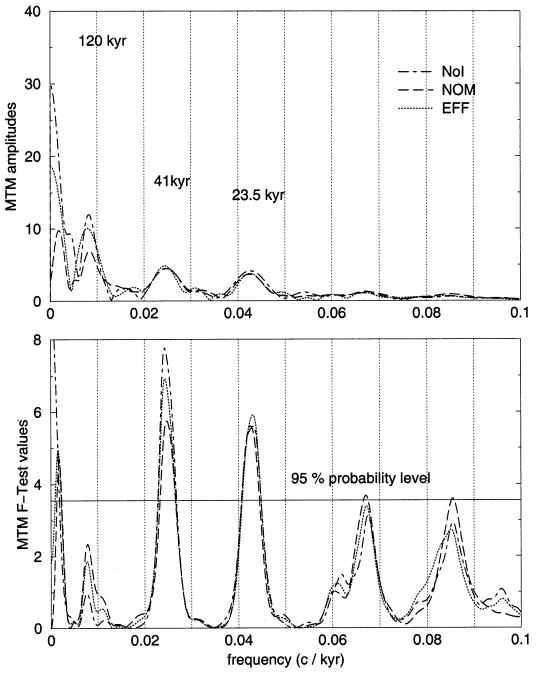

Fig. 4. MTM spectral analysis of simulated NH ice volume for experiments NoI, NOM and EFF. The upper graph displays the amplitude and the lower graph shows *F*-test values (a value of 3.55 corresponds to 95% probability level). Frequencies are expressed in cycles per kyr.

for climate-driven models of ice volume variations over the last 200 kyr. The comparison between experiments NoI (no isostasy) and NOM shows that isostasy acts as a negative feedback during the glaciation process (the rate of ice volume increase is larger when no isostasy is included) and acts as a positive feedback during the deglaciation (in particular, the amplitude of the last deglaciation is considerably underestimated when isostasy is not included). It is possible to understand these features by considering the effect of a change in altitude on the ablation rate over the ice sheet. Indeed, during ice sheet growth, its altitude increases which induces a cooling of the surface air temperature. Hence, ablation (mainly melting) decreases and ice sheet building is enhanced. Actually, the net accumulation rate over the ice sheet is also affected by the decrease in snow precipitation with increasing altitude but this does not affect significantly the feedback loop. On the other hand, this positive altitude feedback is less efficient if the bedrock is deflected under the ice load because the altitude at summit increases less rapidly. This is the reason why the ice volume increases slower in NOM than in NoI. Moreover, the isostatic adjustment is of reduced amplitude if effective parameters are used rather than the nominal ones because the effective density is larger than the nominal density. This explains why the rate of ice volume increase in EFF ranges between NOM and NoI. As previously shown [1], using a high relaxation time is also favorable to ice volume increase, simply because the underlying bedrock takes more time to adjust under ice load and hence the ice sheet altitude increases faster. However, this effect can be considered as a marginal one in the range of relaxation times tested here.

When deglaciation starts, the southward zone of the ice sheet melts very rapidly, as opposed to the top of the ice sheet which is not affected significantly. Consequently, the southward limit of the ice sheet is shifted northward, in regions where the bedrock was strongly depressed during the glaciation and has not yet recovered its equilibrium altitude because of the relaxation time of the lithospheric response. Hence, the altitude of the ablation zone is lower than if no isostasy was considered during the simulation. The low altitude of the ablation zone has a first, straightforward consequence on melting because surface air temperature increases with decreasing altitude. A second effect contributes to the deglaciation process. The low altitude of the ablation zone enhances the southward ice flow towards warm regions because meridional ice velocity is taken proportional to the third power of the meridional altitude gradient (cf. equation 2 in [7]). Consequently, the altitude of the northern part of the ice sheet decreases, until the net ablation, i.e. the ablation minus accumulation, becomes positive everywhere on the ice sheet. From this explanation, it seems that the melting rate should depend on the delay between the northward shift of the ice sheet margin and the response of the underlying bedrock. This delay is taken into account in Eq. 1 by the parameter τ. However, it is shown here that the simulated ice volume is not very sensitive to the difference between nominal and effective τ. This suggests that, using this formalism, differences in lower mantle viscosity between Eurasia and North America should not induce radically different behaviors of these ice sheets in response to a given external forcing.

Although the above process was already described by previous authors (see, e.g. figure 6 in [25]), our simulations stress that the effect of isostasy appears important even for a limited decrease in ice volume as, for example, between 63 and 53 kyr BP. During this period, the volumes of the Northern American and Eurasian ice sheets change significantly only if isostatic rebound is implemented (NOM and EFF). Moreover, the amplitude of these variations is nearly as large in EFF as in NOM, although the density of the mantle is much larger in EFF than in NOM.

Generally, including isostasy improves the quality of the simulated ice volume throughout the last 140 kyr, especially when effective parameters are used. This favorable effect of isostasy is less clear during isotopic stage 6, and NOM, in particular, predicts unrealistic interglacial conditions at 170 kyr BP. But as the simulated ice volume at that time is highly dependent on the initial conditions, longer integrations are needed to examine this earlier part of the model predictions.

5. Conclusion

We have introduced the concepts of effective upper mantle density and relaxation time as an improvement in the classical local damped isostasy formulation used to describe the ice–mantle interaction in simple climate models. They depend on the ice sheet size and the period characterizing the ice load–unload cycle. Sensitivity experiments with the LLN ice-climate model over the last two glacial–interglacial cycles confirm the importance of isostasy on ice volume variations. It appears also that the best results are obtained when effective parameters are applied independently for each ice sheet rather than when nominal parameters are used. Effective density appears as the key parameter and leads to higher ice volumes than in the nominal case. However, using effective τ enhances slightly the deglaciation process because the bedrock takes more time to recover its equilibrium altitude after the LGM. The LLN model also shows that isostasy is necessary to explain ice volume variations during OIS 3, with isostasy exerting a negative feedback on ice volume increase during glaciation processes and a positive feedback on ice volume decrease during deglaciation processes.

Acknowledgements

We thank Tony Purcell (Research School of Earth Sciences, Canberra) who performed the experiments with the RSES Earth Model. Most of this work was performed during a visit by K.L. at the Université catholique de Louvain as invited Professor. M.C. is a research fellow with the National Fund for Scientific Research (Belgium). Comments from Thomas S. James as well as from two anonymous reviewers helped us to improve the original version of the manuscript.*[AC]*

Appendix A. Description of the LLN 2D NH climate model

The climate model used here (designated LLN 2D NH for Louvain-la-Neuve latitude–altitude climate model of the NH) links the NH atmosphere, ocean mixed layer, sea ice, ice sheets and continents. The atmosphere dynamics are simulated by a zonally averaged, two-level quasi-geostrophic model. Eddies are considered as subgridscale processes and are parameterized in a diffusive way. The zonally averaged heating of the atmosphere is made up of the contributions of the convergence of sensible heat transport by the Hadley cells, latent heat release associated with precipitation and the convergence of heat surface fluxes. To compute heat surface fluxes, each latitude belt is divided into at most seven sectors where each one is associated with a surface type: ocean (ice-covered and ice free), continent (snow-covered and snow free) and the main NH ice sheets (the Northern American ice sheet, the Eurasian ice sheet and Greenland). Each sector interacts separately with the atmosphere and the sub-surface. Solar radiation calculation takes into account absorption by H_2O, CO_2 and O_3, Rayleigh scattering, absorption and scattering by clouds and aerosols, and reflection by the surface. Snow free land surface albedo is a function of the water surface availability. Over snow and ice sheets, albedo is a function of snow precipitation frequency, snow surface temperature, solar zenithal angle and the taiga–tundra fraction [26]. The model explicitly incorporates surface energy balance as well as snow surface budget. Sensible and latent vertical heat fluxes are parameterized. The vertical profile of the upper ocean temperature is computed by a mixed-layer model. The ocean transport and its influence on the sea-surface temperature are simulated through a diffusive parameterization of the meridional convergence of heat. Sea ice is represented by a thermodynamic model including leads formation and a parameterization of lateral accretion.

This climate model is asynchronously coupled to a model of the three main NH ice sheets. Ice sheet thickness is deduced from the vertically integrated equation for ice mass conservation. Northward ice velocity obeys the generalized ice flow law from Weertman [27], and mass discharge in the longitudinal direction is parameterized following Oerlemans and Vernekar [28]. The deflection of bedrock under an ice load

is approximated using the local damped isostasy model.

Insolation at the top of the atmosphere is computed following Berger [20]. Analyses of the sensitivity of this model to CO_2 concentration and initial conditions with this model have shown that the broad features of SPECMAP reconstructions are reproduced when CO_2 is constrained by observed data and when no continental ice pre-exists at 200 kyr BP [8].

References

[1] J. Oerlemans, Model experiments on the 100 000-yr glacial cycle, Nature 287 (2) (1980) 430–432.

[2] M. Ghil, H. Le Treut, A climate model with cryodynamics and geodynamics, J. Geophys. Res. 86 (C8) (1981) 5262–5270.

[3] H. Le Treut, M. Ghil, Orbital forcing, climatic interactions and glaciation cycles, J. Geophys. Res. 88 (C9) (1983) 5167–5190.

[4] G. Birchfield, M. Ghil, Climate evolution in the Pliocene and Pleistocene from marine-sediment records and simulations: Internal variability versus orbital forcing, J. Geophys. Res. 98 (D6) (1993) 10385–10399.

[5] L. Tarasov, W. Peltier, A high-resolution model of the 100 ka ice-age cycle, Ann. Glaciol. 25 (1997) 58–65.

[6] H. Gallée, J.P. van Ypersele, T. Fichefet, C. Tricot, A. Berger, Simulation of the last glacial cycle by a coupled, sectorially averaged climate–ice sheet model. Part I: The climate model, J. Geophys. Res. 96 (1991) 13139–13161.

[7] H. Gallée, J.P. van Ypersele, T. Fichefet, I. Marsiat, C. Tricot, A. Berger, Simulation of the last glacial cycle by a coupled, sectorially averaged climate–ice sheet model. Part II: Response to insolation and CO_2 variations, J. Geophys. Res. 97 (1992) 15713–15740.

[8] A. Berger, M.F. Loutre, H. Gallée, Sensitivity of the LLN climate model to the astronomical and CO_2 forcings over the last 200 ky, Clim. Dyn. 14 (1998) 615–629.

[9] L. Pépin, D. Raynaud, J.-M. Barnola, M.F. Loutre, Hemispheric roles of climate forcings during glacial–interglacial transitions, J. Geophys. Res., in press.

[10] W.R. Peltier, Postglacial variations in the level of the sea: Implications for climate dynamics and Solid-Earth geophysics, Rev. Geophys. 36 (4) (1998) 603–689.

[11] E. LeMeur, P. Huybrechts, A comparison of different ways of dealing with isostasy: examples from modeling the Antarctic ice sheet during the last glacial cycle, Ann. Glaciol. 23 (1996) 309–317.

[12] M. Nakada, K. Lambeck, Glacial rebound and relative sea-level variations: a new appraisal, Geophys. J. R. Astron. Soc. 90 (1987) 171–224.

[13] A. Dziewonski, D. Anderson, Preliminary Reference Earth model, Phys. Earth Planet. Int. 25 (1981) 297–356.

[14] K. Lambeck, P. Johnson, M. Nakada, Holocene glacial rebound and sea-level change in NW Europe, Geophys. J. Int. 103 (1990) 451–468.

[15] K. Lambeck, P. Johnston, C. Smither, M. Nakada, Glacial rebound of the British Isles – III: Constraints on mantle viscosity, Geophys. J. Int. 125 (1996) 340–354.

[16] K. Lambeck, C. Smither, P. Johnson, Sea-level change, glacial rebound and mantle viscosity for northern Europe, Geophys. J. Int. 134 (1998) 102–144.

[17] M. Simons, B.H. Hager, Localization of the gravity field and the signature of glacial rebound, Nature 390 (1997) 500–504.

[18] J.X. Mitrovica, A.H. Forte, Radial profile of mantle viscosity: Results from the joint inversion of convection and postglacial rebound observables, J. Geophys. Res. 102 (1997) 2751–2769.

[19] G. Kaufmann, K. Lambeck, Mantle dynamics, postglacial rebound and the radial viscosity profile, Phys. Earth Planet. Int. 121 (3–4) (2000) 303–327.

[20] A. Berger, Long-term variations of daily insolation and Quaternary climatic changes, J. Atmos. Sci. 35 (1978) 2362–2367.

[21] J. Jouzel, N.I. Barkov, J.-M. Barnola, M. Bender, J. Chappellaz, C. Genthon, V.M. Kotlyakov, C. Lorius, J.-R. Petit, D. Raynaud, G. Raisbeek, C. Ritz, T. Sowers, M. Stievenard, F. Yiou, P. Yiou, Vostok ice cores: extending the climatic records over the penultimate glacial period, Nature 364 (6436) (1993) 407–412.

[22] J. Imbrie, D. Hays, D. Martinson, A. McIntyre, A.C. Mix, J.J. Morley, N.G. Pisias, W.L. Prell, N.J. Shackleton, The orbital theory of Pleistocene climate: Support from a revised chronology of the marine $\delta^{18}O$ record, in: A. Berger, J. Imbrie, J. Hays, G. Kukla, B. Saltzman (Eds.), Milankovitch and Climate, Part I, D. Reidel, Norwell, MA, 1984, pp. 269–305.

[23] D.J. Thomson, Spectrum estimation and harmonic analysis, IEEE Proc. 70 (1982) 1055–1096.

[24] J.-R. Petit, J. Jouzel, D. Raynaud, N.I. Barkov, J.-M. Barnola, I. Basile, M. Bender, J. Chappellaz, M. Davis, G. Delaygue, M. Delmotte, V.M. Kotlyakov, M. Legrand, V.Y. Lipenkov, C. Lorius, L. Pépin, C. Ritz, E. Saltzman, M. Stievenard, Climate and atmospheric history of the past 420 000 years from the Vostok ice core, Antarctica, Nature 399 (6735) (1999) 429–436.

[25] W.R. Peltier, Glacial isostasy, mantle viscosity and Pleistocene climatic change, in: W. Ruddiman, H. Wright (Eds.), North America and Adjacent Oceans during the Last Deglaciation, Vol. K-3 of Geology of North America, The Geological Society of America, Boulder, Co., 1987, pp. 155–182.

[26] L.D.D. Harvey, On the role of high latitude ice, snow and vegetation feedbacks in the climatic response to external forcing changes, Clim. Change 13 (1988) 191–224.

[27] J. Weertman, Creep of ice, in: E. Whalley, S. Jones (Eds.),

Physics and Chemistry of Ice, Royal Society of Canada, Ottawa, 1973.
[28] J. Oerlemans, A.D. Vernekar, A model study of the relation between northern hemisphere glaciation and precipitation rates, Beitr. Phys. Atmos. 54 (1981) 352–361.
[29] W.R. Peltier, S. Marshall, Coupled energy-balance/ice-sheet model simulations of the glacial cycle: A possible connection between terminations and terrigenous dust, J. Geophys. Res. 100 (D7) (1995) 14269–14289.
[30] G.E. Birchfield, J. Weertman, A. Lunde, A paleoclimate model of Northern Hemisphere ice sheets, Quat. Res. 15 (1981) 126–142.
[31] B.U. Neeman, G. Ohring, J.H. Joseph, The Milankovitch theory and climate sensitivity 2. Interaction between the Northern Hemisphere ice sheets and the climate system, J. Geophys. Res. 93 (D8) (1988) 11175–11191.
[32] R.S. Bradley, Paleoclimatology, Reconstructing the Climates of the Quaternary, Vol. 64 of International Geophysics Series, Academic Press, 1999, 613 pp.